ELSEVIER

Carbohydrate Research 305 (1998) 261–269

CARBOHYDRATE RESEARCH

The enzymatic susceptibility of cellulose microfibrils of the algal–bacterial type and the cotton–ramie type

Noriko Hayashi [a,*], Junji Sugiyama [b], Takeshi Okano [c], Mitsuro Ishihara [a]

[a] *Forestry Forest Products Research Institute, P.O. Box 16, Tsukuba Norin Kenkyu Danchi-nai, Ibaraki 305, Japan*

[b] *Wood Research Institute, Kyoto University, Uji, Kyoto 611, Japan*

[c] *Faculty of Agriculture, The University of Tokyo, Yayoi 1-1-1, Bunkyo-Ku, Tokyo 113, Japan*

Received 23 September 1996; accepted 8 September 1997

Abstract

Two types of substrates, the algal–bacterial type (rich in cellulose I_α) cellulose and the cotton–ramie type (dominant in cellulose I_β) cellulose, were degraded comparatively by *Trichoderma viride* cellulase. The algal–bacterial type cellulose microfibril was more susceptible than the cotton–ramie type. The residual cellulose microfibrils were observed by TEM and analyzed by FTIR and electron diffraction. It becomes clear that the residual cellulose of the algal–bacterial type cellulose was getting rich in the cellulose I_β with the lapse time of cellulase treatment. These results indicate that the cellulose I_α in the microfibril of the algal–bacterial type cellulose is hydrolyzed preferentially by the cellulase. © 1998 Elsevier Science Ltd

Keywords: Cellulose, algal–bacterial type; Cellulose, cotton–ramie type; Cellulase; Cellulose I_α; Microfibril

1. Introduction

The cellulase system from potent cellulolytic fungi such as *Trichoderma* species possesses endo-(1 → 4)-β-D-glucanases attacking randomly within the cellulose chain, exo-(1 → 4)-β-D-glucanases splitting either cellobiose or glucose from the non-reducing end of cellulose, and a β-D-glucosidase that converts cellobiose and other cello-oligosaccharides to glucose [1,2].

The enzymatic hydrolysis of cellulose, particularly hydrogen-bonded and ordered crystalline cellulose, is a very complex process. As the cellulose is insoluble, the cellulases must diffuse and fit themselves to the structural features of the substrate. A number of investigators regarded the crystallinity, the surface accessibility and the particle size of cellulosic substrates as the major factors affecting enzyme hydrolysis [3]. The relationship between the fine structural features and the digestibility in cellulosic materials should be clarified, not only for achieving effective glucose production, but also for better understanding of the reaction mechanism.

* Corresponding author.

PII S0008-6215(97)10032-5

Marrinan and Mann [4] indicated the difference of the cellulose crystals. Recent investigations have revealed that native cellulose crystals are the composite of two different crystalline components, cellulose I_α and cellulose I_β, and that cellulose I_α is rich in the algal–bacterial type celluloses, whereas cellulose I_β is dominant in the cotton–ramie type celluloses [5–10]. Furthermore, the following information has also been obtained: (1) Cellulose I_α and cellulose I_β should have different hydrogen-bonding systems. The difference was first demonstrated by Raman spectroscopy [7–10] and also confirmed by FTIR spectroscopy [11,12]. (2) Cellulose I_α can be transformed into cellulose I_β by hydrothermal annealing in the presence of NaOH; therefore, cellulose I_β is thermodynamically more stable than cellulose I_α [13–15]. (3) Cellulose I_β from the tunic of *Halocynthia* sp. exists in a pure I_β phase [16]. (4) Cellulose I_α and cellulose I_β are characterized as crystals consisting of a one-chain triclinic unit cell and a two-chain monoclinic unit cell, respectively, and the theoretical density of the monoclinic unit cell is slightly larger than that of the triclinic unit cell [17]. (5) Hackney et al. [18] and Uhlin et al. [19] also suggested the presence of a superlattice-like structure, in which the cellulose I_α and cellulose I_β domains coexist throughout the cross-section of each microfibril. (6) It is noteworthy that cellulose I_β is dominant in wood cell walls [20].

The accessibility of cellulose dimorphs (I_α/I_β) to chemicals as well as biochemical reactions has been far less studied in comparison to their structural characterization. Atalla and VanderHart reported in the acid hydrolysis residue of highly crystalline cellulose from *Rhizoclonium heiroglyphicum* and *Cladophora gromerata* investigated by solid-state CPMAS ^{13}C NMR spectroscopy, that in the *Rhizoclonium*, cellulose I_α and cellulose I_β were equally susceptible to acid hydrolysis [21], but in *Cladophora*, cellulose I_α was degraded more rapidly than cellulose I_β [10]. Kim and Newman [22] suggested from ^{13}C NMR analysis that cellulose I_α was preferentially degraded in brown rot decay of Korean red pine. Both results suggested that the cellulose I_α component is more accessible, but that fact was not clearly established. In this paper, we conducted quantitative analysis on the susceptibility of *Trichoderma viride* cellulase to the dimorphs in the microfibrils of various native celluloses. For this, the enzymatic susceptibility was examined by the weight loss during the degradation process, and the hydrolysis residues were analyzed by FTIR spectroscopy and by electron diffraction.

2. Experimental

Substrates.—Two types of substrates were used. One was (a) the algal–bacterial type cellulose that is rich in cellulose I_α: bacterial (*Acetobacter xylinum*) cellulose gel, cell walls of *Valonia* sp. harvested from Wakayama, Japan, and *Cladophora* sp. collected in Chiba, Japan. The other was (b) the cotton–ramie type cellulose that is dominant in cellulose I_β: tunic of *Halocynthia* sp. commercially obtained, cotton linter pulp (dp 3500), bleached softwood pulp (dp 750 and 1500), bleached hardwood pulp (dp 1500), and Avicel (PH-101, Asahi Chemical). Purification for some of the samples was needed to remove noncellulosic substances, and homogenization was carried out to avoid the aggregation of cellulose microfibrils. The pellicles of bacterial cellulose were purified by boiling in 1% NaOH for 10 h under a stream of nitrogen gas, then washing with distilled water [23], homogenization into small fragments, and freeze-drying. The vesicles of *Valonia* sp. were purified by the procedure of Gardner and Blackwell [24] and treated acid-mechanically by the method of Chanzy and Henrissat [25]. The tunic of *Halocynthia* sp. was repeatedly bleached in 0.3% sodium chlorite in acetate buffer, pH 4.9. This sample was left in 5% KOH overnight and washed thoroughly with distilled water [15], and then homogenized into small fragments and freeze-dried. Avicel was boiled in 2.5 N HCl for 15 min and thoroughly washed with distilled water.

Enzymatic hydrolysis.—All the samples were hydrolyzed with a commercial enzyme 'Meicelase' (Meiji Seika Kaisha, Tokyo, Japan) derived from *T. viride*. The enzyme preparation had 0.40 U/mg of filter paper degrading activity, 4.9 U/mg of CMC-Na degrading activity and 0.94 U/mg of cellobiase activity. The substrate (200 mg) in 10 mL of 0.1 M NaOAc buffer (pH 4.8) was incubated with enzyme (50 mg) at 40 °C for 2 days, except for the bacterial cellulose. The bacterial cellulose was incubated for 0.5 and 1 h because this sample was quite degradable with cellulase. The reaction mixture was separated by centrifugal separation into the residues and products. The precipitate was thoroughly washed with 0.1 N NaOH solution and distilled water, then freeze-dried and weighed. The enzymatic susceptibility was calculated as ratio of weight loss to the initial sample weight. This treatment was repeated twice or more replacing cellulase solution until the samples were hydrolyzed about 80–90% from initial weight on each residue of the *Cladophora* and *Halocynthia*

cellulose, that have almost the same crystal dimensions. This treatment was also repeated on the residues of *Valonia*.

Hydrothermal treatment.—Some bacterial cellulose was subjected to hydrothermal treatment. The purified and homogenized cellulose sample was inserted into a glass ampule with a small amount of 0.1 N NaOH. This sample was sealed and placed in an autoclave at 260 °C for 30 min, then cooled in tap water. The annealed sample was washed thoroughly with distilled water and then freeze-dried. This sample was also treated with cellulase in the same fashion. The samples before and after hydrothermal treatment showed almost the same crystallinity.

Observation by TEM.—Some of the freeze-dried residues were suspended in water. A drop from each suspension was deposited on a carbon-coated grid and observed with the transmission electron microscope (TEM; JEM-2000EX, JEOL, Japan) with staining of 1.5% uranyl acetate for imaging. The results were recorded on Mitsubishi electron microscopic films (MEM).

FTIR spectral analysis.—FTIR spectra were obtained from the samples mounted on a potassium bromide disk using an FTIR instrument equipped with an ordinal microscopic accessory (Nicolet-Magna 550 FT-IR, France). The wave number range scanned was 3800–650 cm^{-1}, 64–200 scans of 4 cm^{-1} resolution were signal averaged and stored.

X-ray and electron diffraction.—From the characterization of the cellulose I_α (triclinic) component and cellulose I_β (monoclinic) component, $(1\bar{1}0)$, (110) and (200) planes in the two-chain monoclinic unit cell are, respectively, equivalent to (100), (010) and (110) planes in the one-chain triclinic unit cell [17]. Here, we used the monoclinic indices to represent the Millar's indices of the two crystal systems. X-ray diffraction profiles were obtained with a JDX-8200 (JEOL, Japan) instrument. The separation of peaks in X-ray profiles was carried out using a least-squares refinement program by the method of Wada et al. [26]. The diffraction angle was calibrated for each run with titanium oxide ($d = 0.2487$ nm). The crystal dimensions of three main equatorial reflections of cellulose, which were $(1\bar{1}0)$, (110) and (200) planes, respectively, were determined using Sherrer's equation [27]. The crystallinity indices (CrI) of the initial samples were calculated from X-ray profiles by the

Table 1
The change of weight loss, crystal dimension and ratio of I_α:I_β on various native celluloses before and after the enzymatic treatment

Sample (CrI (%))	Time course	Weight loss (%)	Crystal dimension (nm)			Ratio of I_α:I_β (%)
			$1\bar{1}0$	110	200	
Valonia	0 day	0	14.8	16.9	23.0	34/66
(87)	2	46	14.8	16.9	23.0	16/84
Cladophora	0 day	0	11.0	9.2	14.3	54/46
(82)	2	52	10.5	9.1	11.0	50/50
Bacterial	0 h	0	6.2	6.4	6.3	44/56
(69)	0.5	68	5.7	6.2	6.1	26/74
	1.0	97	6.3	5.9	5.3	
Halocynthia	0 day	0	7.9	8.7	10.0	
(86)	2	38	8.0	8.5	9.6	
Cotton linter	0 day	0	5.8	6.5	6.0	
(73)	2	44	6.3	6.3	6.1	
Avicel (HCl)	0 day	0	–	–	4.4	
(63)	2	40	–	–	4.7	
Soft wood Pulp (dp = 1000) (61)	0 day	0	–	–	4.6	
	2	39	–	–	4.3	
Soft wood Pulp (dp = 2100) (59)	0 day	0	–	–	4.6	
	2	37	–	–	4.7	
Hard wood Pulp (dp = 900) (56)	0 day	0	–	–	3.9	
	2	37	–	–	4.1	

method of von Knolle and Jayme [28]. For electron diffraction, the samples prepared above for TEM observation were used without any treatment or shadowed by gold.

3. Results

Table 1 shows the changes of weight loss, crystal dimension and the changes in the composition of cellulose I_α and cellulose I_β after enzymatic treatment for 2 days, except for the bacterial cellulose that was examined after 0.5 and 1 h of enzymatic treatment. The peaks of $(1\bar{1}0)$ and (110) planes from the profiles of Avicel and pulp samples could not be separated, and the crystal dimensions of the $(1\bar{1}0)$ and (110) planes were not calculated.

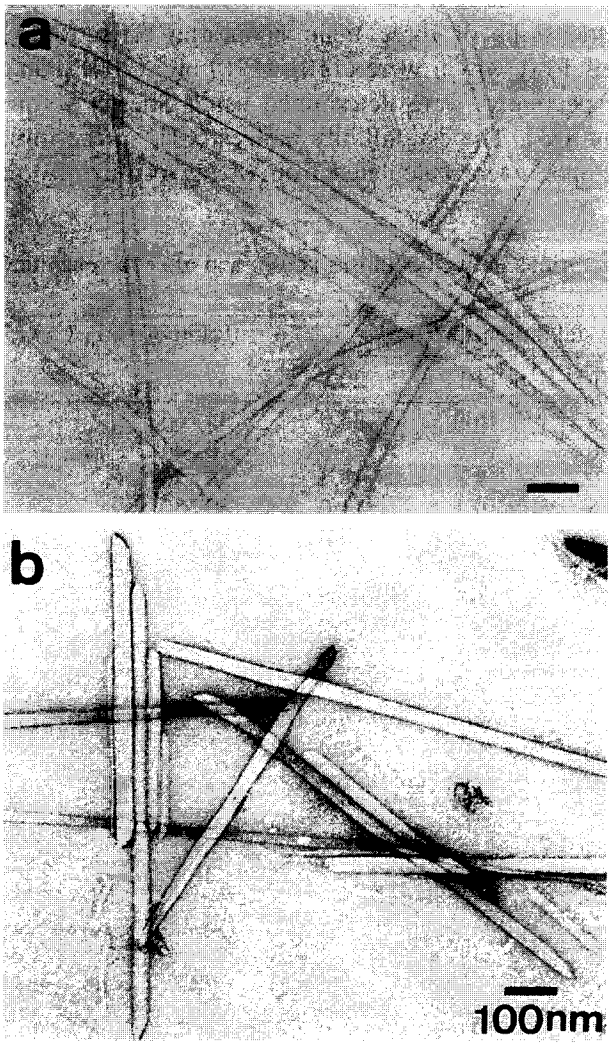

Fig. 1. The electron micrographs of the *Cladophora* cellulose microfibrils: (a) control, (b) after 2 days of enzymatic treatment.

It was also noted that short microfibrils became prominent during the enzymatic hydrolysis from the TEM observation of the residual *Cladophora* cellulose (Fig. 1).

4. Discussion

The results of the weight loss in various cellulose samples suggested that the algal–bacterial type cellulose microfibrils seemed to be more degradable than the cotton–ramie type.

It is interesting that the bacterial cellulose was hydrolyzed with enzymes quite easily. We compared the bacterial cellulose microfibril under different conditions: (a) control; (b) after hydrolysis with CBH I purified from the Meicelase, which was a main component of the *T. viride* cellulase, for 10 min and then ultrasonic treatment for 10 min; (c) ultrasonic treatment for 20 min. The results were shown in Fig. 2a–c. The untreated microfibrils were not fibrillated (Fig. 2a), but after enzymatic treatment, the microfibril was fibrillated uniformly into bundles of thin subfibrils and sometimes became short subfibrils (Fig. 2b). The microfibrils under only ultrasonic treatment were not different from the control sample, but partly fibrillated (Fig. 2c). White [29] and Brown et al. [30] also reported the fibrillation of the ribbon of bacterial cellulose in the enzymatic degradation process. The ribbon-like structure of bacterial cellulose microfibril will be fibrillated easily by the enzymatic attack. If the breakdown of the bonding between subfibrils is mediating the enzyme, the resulting increase of the surface in the thinned subfibrils should be effective for enzymatic attack. The rapid fibrillation in such a short incubation was not observed in the other cellulose samples. This might be the reason for the high degradability of the bacterial cellulose microfibrils and the bacterial cellulose should be a unique substrate for cellulase.

The CrI and surface area have been considered to be important factors for determining enzymatic susceptibility. Therefore, we compared the CrI of cellulose substrates before the enzymatic treatment (Table 1). In the algal–bacterial type cellulose, the CrI of bacterial cellulose was 69%, *Cladophora*, 82%, and *Valonia*, 87%. In the algal–bacterial type cellulose, there was a reasonable relationship between the CrI and the enzymatic susceptibility, namely, the lower CrI of the sample was the more susceptible it was to enzymatic attack. In the cotton–ramie type cellulose,

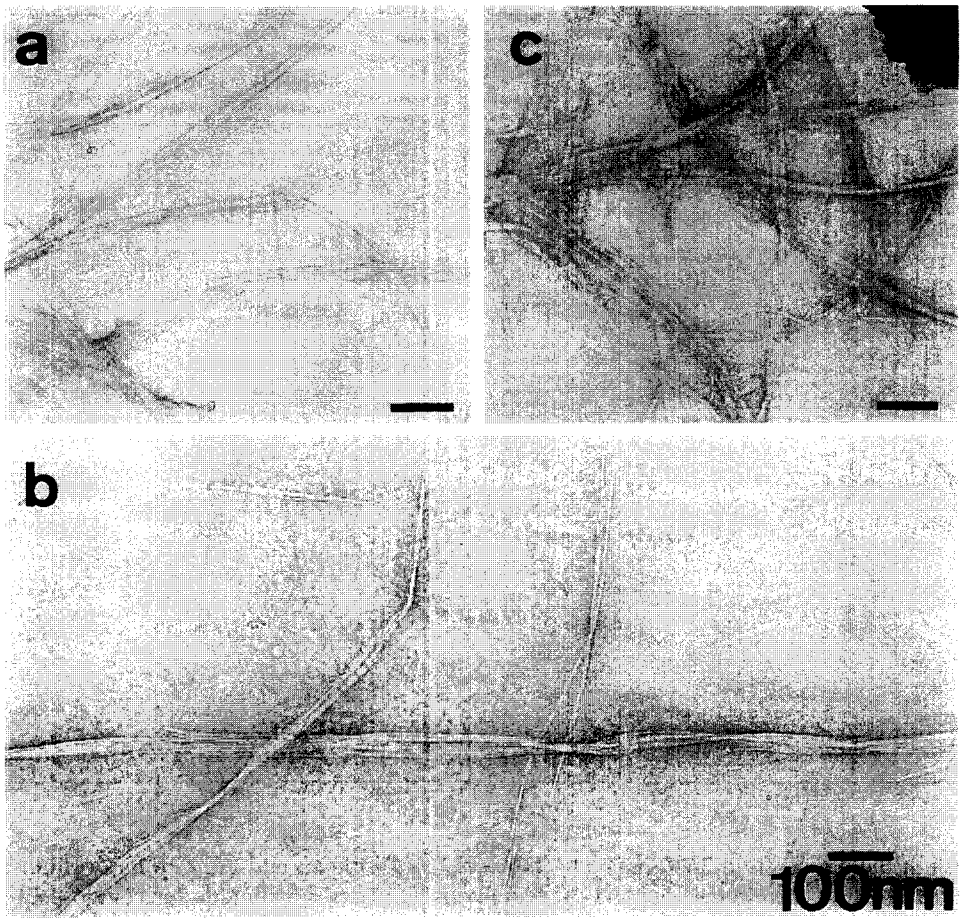

Fig. 2. The electron micrographs of the bacterial cellulose microfibrils: (a) control; (b) after hydrolysis with CBH I purified from the Meicelase, for 10 min and then treated with ultrasonic for 10 min; (c) ultrasonic treatment for 20 min without enzymatic hydrolysis.

the CrI of *Halocynthia* cellulose was 86%; cotton linter pulp, 73%; acid-treated Avicel, 69%; softwood pulp, 60%; and hardwood pulp, 56%. There was not a similar correlation to the cotton–ramie type between the enzymatic susceptibility and the CrI. We previously reported that the size of the cellulose crystallites and aggregation of cellulose microfibrils should play a major role in the enzymatic susceptibility of the cotton–ramie type cellulose [31]. Compared with the two types of cellulose, although the CrIs and surface areas (crystal dimension) of the algal–bacterial type celluloses were higher than those of the cotton–ramie type, the enzymatic susceptibility of the algal–bacterial type cellulose was higher than that of the cotton–ramie type.

Hydrothermal treatment transforms cellulose I_α into cellulose I_β [13–15]. The effects of annealing on the enzymatic susceptibility of bacterial cellulose were

Fig. 3. The electron micrograph of the bacterial cellulose after the hydrothermal treatment under NaOH.

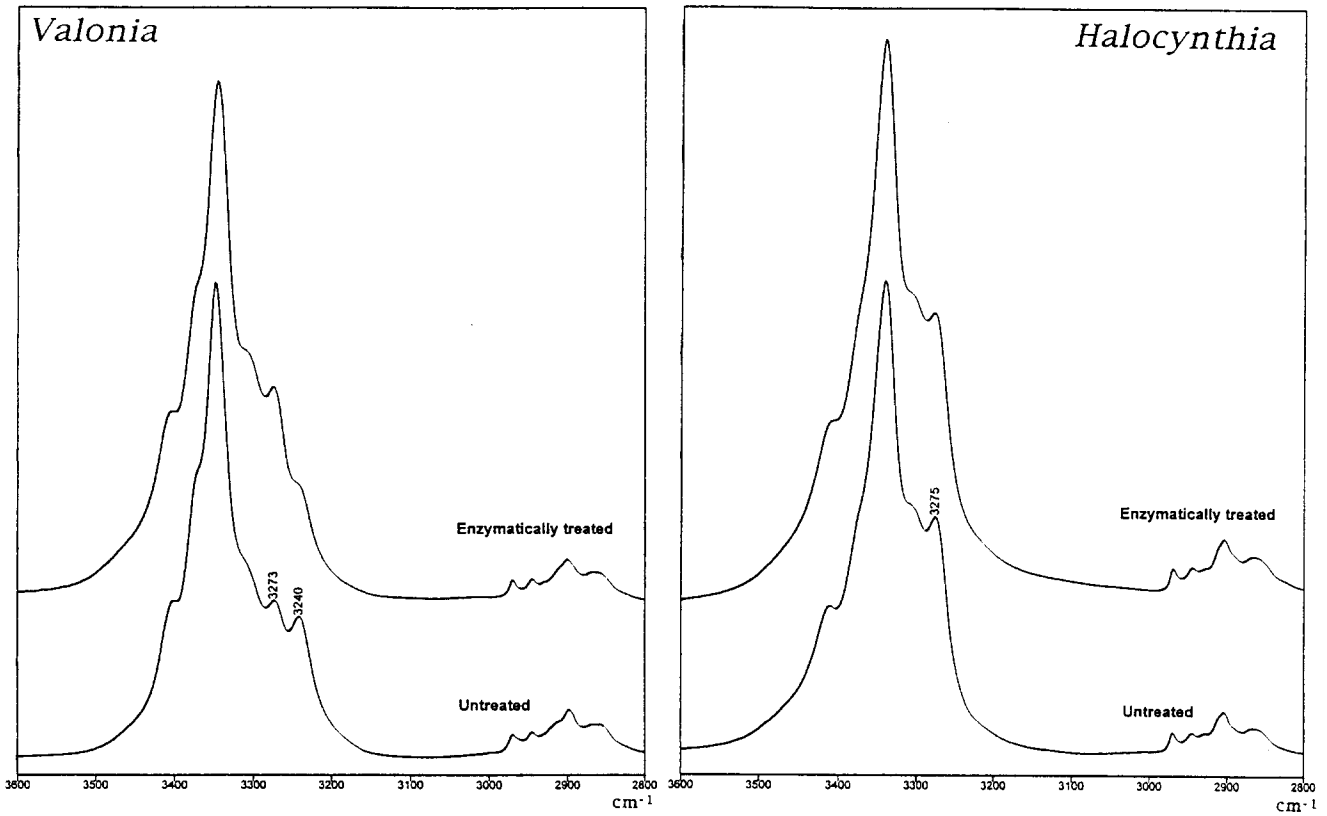

Fig. 4. FTIR spectra in the region from 3600 cm^{-1} to 2800 cm^{-1} of *Valonia* and *Halocynthia* celluloses. Note: the band near 3240 cm^{-1} is assigned as to cellulose I_α, and the band near 3270 cm^{-1} is unique for cellulose I_β.

studied. The morphological change of the annealed bacterial cellulose is shown in Fig. 3. The microfibrils were observed to shorten but not to form tight aggregation. The CrI was not changed after the annealing. After a 1-h enzymatic treatment, the weight losses of the unannealed and annealed bacterial cellu-

Table 2
The changes of weight loss, *d*-spacings and ratio of I_α:I_β of the residues of *Cladophora* and *Halocynthia* during the successional enzymatic hydrolysis

Sample	Time course	Weight loss (%)	*d*-Spacing (nm)			Ratio of I_α:I_β (%)
			$(1\bar{1}0)$	(110)	(200)	
Cladophora	0 day		0.612	0.519	0.386	54/46
	2	52	0.599	0.523	0.387	50/50
	2 + 4	60	0.597	0.521	0.387	39/61
	2 + 4 + 2	69	–	–	–	
	2 + 4 + 2 × 2	75	0.599	0.522	0.387	36/64
	2 + 4 + 2 × 3	79	0.599	0.525	0.387	40/60
	2 + 4 + 2 × 4	82	0.602	0.526	0.388	37/63
Halocynthia	0 day		0.593	0.529	0.386	
	2 × 1	40	0.591	0.529	0.386	
	2 × 2	65	0.594	0.531	0.386	
	2 × 3	78	0.591	0.528	0.386	
	2 × 4	85	0.594	0.529	0.386	
	2 × 5	88	0.594	0.529	0.386	
	2 × 6	90	0.593	0.528	0.386	

lose was 91% and 56%, respectively. As described before, bacterial cellulose was a highly degradable substrate, but the conversion of cellulose I_α to cellulose I_β seemed to inhibit the enzymatic hydrolysis. We, therefore, considered that the crystalline dimorphs (I_α/I_β) might have much more influence on the enzymatic action on the crystalline cellulose rather than the CrI and surface area from the viewpoint of cellulose crystals.

The composite make-up of the residual cellulose was clarified with FTIR absorption and TEM diffraction. In Fig. 4, the IR spectrum around the region of 3600–2800 cm^{-1} of *Valonia* and *Halocynthia* cellulose samples is compared before and after the enzymatic treatment, respectively. The absorption band in the FTIR spectrum near 3240 cm^{-1} is assigned to the cellulose I_α, whereas the absorption band near 3270 cm^{-1} is assigned to the cellulose I_β [11,12]. *Halocynthia* cellulose did not show any absorption at 3240 cm^{-1}, regardless of enzymatic treatment. On the other hand, the absorption band at 3240 cm^{-1} in *Valonia* cellulose decreased after 60 h of enzymatic treatment. This decrease and disappearance of the absorption band in *Cladophora* cellulose were also observed in the specimens after the enzyme hydrolysis. It is shown in Fig. 5 that the absorption band at about 3240 cm^{-1} in the unannealed bacterial cellulose remarkably decreased after 1 h of enzymatic treatment (Fig. 5a), and in annealed bacterial cellulose, the absorption band at 3240 cm^{-1} disappeared, and the cellulase seemed to have little effect on the cellulose crystalline phase (Fig. 5b).

The changes in the composition of cellulose I_α and cellulose I_β of the algal–bacterial type cellulose were calculated from the peak height of 750 cm^{-1} and 710 cm^{-1} according to the method of Yamamoto et al. [32]. In the residual cellulose, cellulose I_β became rich (Table 1). In *Cladophora* cellulose, cellulose I_β was twice as much as cellulose I_α with increasing cellulase treatment (Table 2).

The changes of the *d*-spacings of the residues of *Cladophora* and *Halocynthia* during the successive enzymatic hydrolysis are shown as $(1\bar{1}0)$, (110) and (200) planes in the Table 2. The *d*-spacings from each crystalline phase were reported, the I_α (triclinic) component: $d_{100} = 0.621$ nm, $d_{010} = 0.528$ nm, $d_{110} = 0.397$ nm; the I_β (monoclinic) component: $d_{1\bar{1}0} = 0.607$ nm, $d_{110} = 0.535$ nm, $d_{200} = 0.398$ nm [17]. It

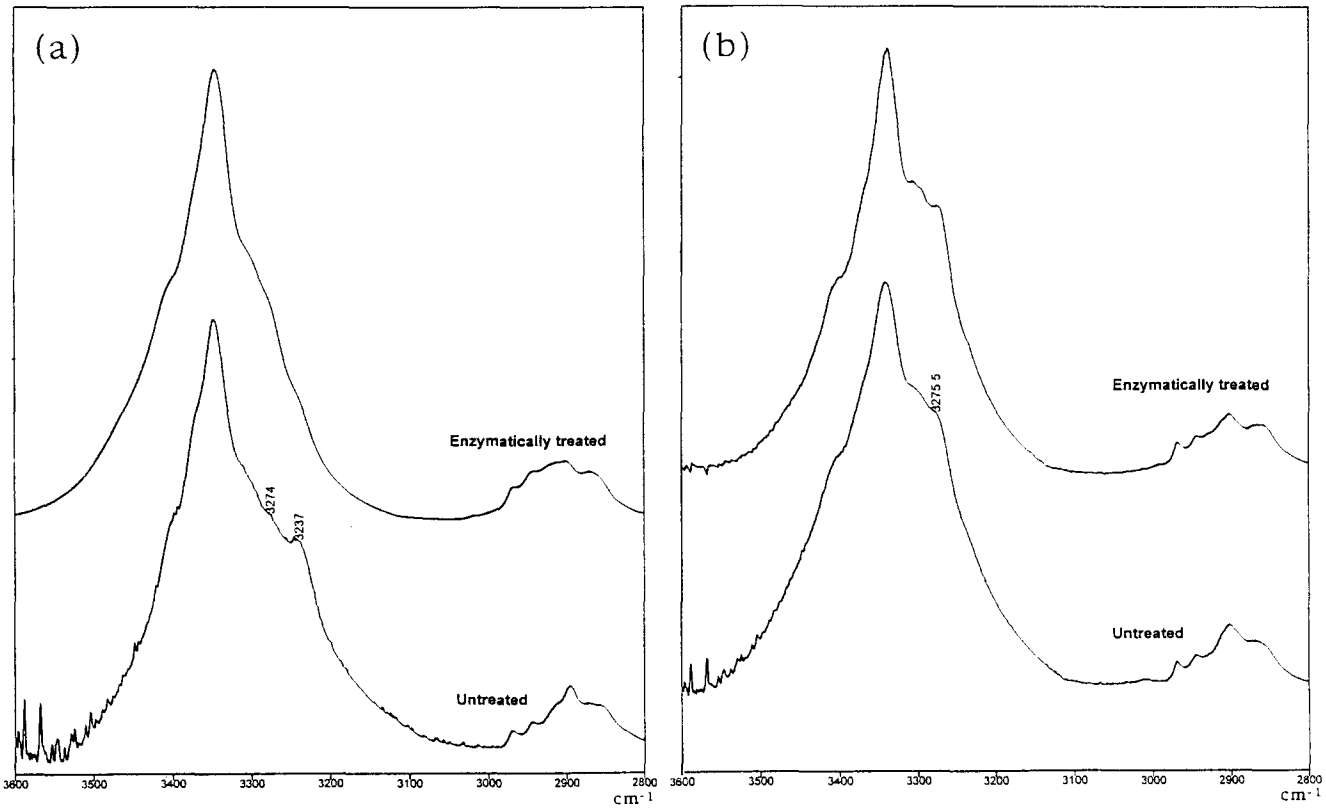

Fig. 5. FTIR spectra in the region from 3600 cm^{-1} to 2800 cm^{-1} of (a) unannealed and (b) annealed bacterial cellulose before and after enzymatic hydrolysis for 1 h.

is noted that d_{100} is larger than $d_{1\bar{1}0}$, and d_{010} is smaller than d_{110}. The *d*-spacings of the residues of the *Halocynthia* cellulose did not change during enzymatic degradation. The d_{100} ($d_{1\bar{1}0}$ in Table 2) of the residues of *Cladophora* cellulose became smaller, but the d_{010} (d_{110} in Table 2) became larger than the initial. This was also observed in the residual cellulose of *Valonia*, so that it was also confirmed by the *d*-spacings that the residual algal–bacterial type celluloses tended to become close to those of the I_β phase in the advanced stages of enzymatic hydrolysis.

As shown in Figs. 4 and 5 and in Table 2, the results of the FTIR absorption and electron diffraction diagrams indicate that the hydrolysis residues of the algal–bacterial type cellulose in the advanced stages of enzymatic hydrolysis were almost cellulose I_β. It is suggested that the cellulose I_α in the algal–bacterial cellulose microfibrils is hydrolyzed preferentially with cellulase: that is, cellulose I_β is rather stable to the cellulase attack in comparison with cellulose I_α. It is also considered that the preferential attack of the cellulase to the cellulose I_α might be caused by the structural differences of the crystalline dimorphs (I_α/I_β) such as the *d*-spacings, the theoretical density and the distribution of the two crystalline phases in the microfibril.

Enzymatic susceptibility

Algal-bacterial type cellulose (rich in cellulose Iα) > **Cotton-ramie type cellulose (rich in cellulose Iβ)**

Why? Because of selective degradation of cellulose Iα.

In the residual *Cladophora* cellulose, short microfibrils became prominent during the enzymatic hydrolysis (Fig. 1). When the bacterial cellulose was treated with CBH I and ultrasonic waves, cutting into same length was partly observed in the resulting subfibrils. Therefore, short microfibrils were thought to be once formed in the enzymatic degradation of the algal–bacterial type cellulose. The formation of short microfibrils might be related to the composition of cellulose dimorphs (I_α/I_β) in the microfibril, and we have discussed these findings in the previous paper [33]. These results did not preclude the presence of superlattice-like structure demonstrated by Atalla et al. It is also suggested that the blocks composed mainly by cellulose I_β may exist in the cellulose microfibril of the algal–bacterial type. It was observed that the residual cellulose microfibrils of the cotton–ramie type became thinner and fibrillated with the progress of the enzyme treatment, and the formation of the short microfibrils did not occur as described in our other paper [31].

The conclusions are summarized as follows: (i) algal–bacterial type cellulose is more susceptible to the enzymatic attack than cotton–ramie type cellulose; (ii) cellulose I_α crystalline phase of the algal–bacterial type cellulose is degraded preferentially by *T. viride* cellulase and the residues become cellulose I_β phase dominant; and (iii) in the degradation process of algal–bacterial type cellulose, shortened microfibrils are observed. Further investigation is necessary to understand why the preferential degradation occurred in the two cellulose dimorphs.

Acknowledgements

The authors thank Dr. T. Kondo of the Forestry and Forest Products Research Institute for his useful critical discussion. The authors thank Prof. A. Kai, Tokyo Metropolitan University, for the gift of bacterial cellulose, Mr. S. Ui, Kushimoto Kaichu Park, for the gift of *Valonia* cellulose, and Mr. M. Wada, the University of Tokyo, for the gift of *Cladophora* cellulose and for his help for the interpretation of X-ray analysis. The authors also thank Dr. N. Matsumoto at the laboratory of Jenssen for technical help in the FTIR analyses.

References

[1] T.C. Wood and S.I. McCrae, *Adv. Chem. Ser.*, 1981 (1979) 181–209.
[2] D.E. Eveleigh, in A.L. Demain and N. Solomon (Eds.), *Trichoderma in the Biology of Industrial Microorganisms*, Benjamin/Cummings Publishing, MenloPark, CA, USA, 1985, pp. 487–509.
[3] L.P. Walker and D.B. Wilson, *Bioresource Technol.*, 36 (1991) 3–19.
[4] J. Marrinan and J. Mann, *J. Polym. Sci.*, 21 (1956) 301–311.
[5] R.H. Atalla and D.L. VanderHart, *Science*, 223 (1984) 283–285.
[6] D.L. VanderHart and R.H. Atalla, *Macromolecules*, 17 (1984) 1472–1479.
[7] J.H. Wiley and R.H. Atalla, *Carbohydr. Res.*, 160 (1987) 113–129.
[8] J.H. Wiley and R.H. Atalla, in R.H. Atalla (Ed.), *The Structures of Cellulose*, ACS Symp. Ser., 340 (1987) 152–168.
[9] F. Horii, A. Hirai, and R. Kitamaru, *Macromolecules*, 20 (1987) 2117–2122.

[10] R.H. Atalla and D.L. VanderHart, in C. Schuerch (Ed.), *Cellulose and Wood-Chemistry and Technology*, Wiley, 1989, 169–188.
[11] A.J. Michell, *Carbohydr. Res.*, 197 (1990) 53–60.
[12] J. Sugiyama, J. Persson, and H. Chanzy, *Macromolecules*, 24 (1991) 2461–2466.
[13] F. Horii, H. Yamamoto, R. Kitamaru, M. Tanahashi, and T. Higuchi, *Macromolecules*, 20 (1987) 2946–2949.
[14] H. Yamamoto, F. Horii, and H. Odani, *Macromolecules*, 22 (1989) 4132–4134.
[15] J. Sugiyama, T. Okano, H. Yamamoto, and F. Horii, *Macromolecules*, 23 (1990) 3196–3198.
[16] P.S. Belton, S.F. Tanner, N. Cartier, and H. Chanzy, *Macromolecules*, 22 (1989) 1615–1617.
[17] J. Sugiyama, R. Vuong, and H. Chanzy, *Macromolecules*, 24 (1991) 4168–4175.
[18] J.M. Hackney, R.H. Atalla, and D.L. VanderHart, *Int. J. Biol. Macromol.*, 16 (1994) 215–218.
[19] K.I. Uhlin, R.H. Atalla, and N.S. Thompson, *Cellulose*, 2 (1995) 129–144.
[20] M. Wada, J. Sugiyama, and T. Okano, *Mokuzai Gakkaishi*, 40 (1994) 50–56; *Chem. Abstr.*, 123 (1995) 138855x.
[21] R.H. Atalla and R.E. Whitmore, *Biopolymers*, 24 (1985) 421–423.
[22] Y.S. Kim and R.H. Newman, *Holzforschung*, 49 (1994) 109–114.
[23] A. Kai and P. Xu, *Polym. J.*, 22 (1990) 955–961.
[24] K.H. Gardner and J. Blackwell, *Biopolymers*, 13 (1974) 1975–2001.
[25] H. Chanzy and B. Henrissat, *Carbohydr. Polym.*, 3 (1983) 161–173.
[26] M. Wada, J. Sugiyama, and T. Okano, *J. Appl. Polym. Sci.*, 49 (1993) 1491–1496.
[27] D. Sherrer, *Gotti. Nachrich.*, 2 (1918) 98.
[28] H. von Knolle and G. Jayme, *Das Papier*, 19 (3) (1965) 106–111.
[29] A.R. White, in R.M. Brown Jr. (Ed.), *Cellulose and Other Natural Polymer Systems: Biogenesis, Structure, and Degradation*, Plenum, New York, 1982, pp. 489–509.
[30] R.M. Brown Jr., C.H. Haigler, J. Suttie, A.R. White, E. Roberts, C. Smith, T. Itoh, and K. Cooper, *J. Appl. Polym. Sci., Appl. Polym. Sympos.*, 37 (1983) 33–78.
[31] N. Hayashi, M. Ishihara, and K. Shimizu, *Mokuzai Gakkaishi*, 41 (1995) 1132–1138; *Chem. Abstr.*, 124 (1996) 205311c.
[32] H. Yamamoto, R. Hirai, and F. Horii, *Proc. of '94 Cellulose R&D*, (1994) 43–44.
[33] N. Hayashi and T. Kondo, *Preprints of '95 Cellulose R&D*, (1995) 77–78.